Experimental Validation of Leak and Water-ingression Detection in Low-Pressure Gas Pipeline Using Pressure and Flow Measurements

Ravula, Sugunakar Reddy; Narasimman, Srivathsan Chakaravarthi; Wang, Libo; Ukil, Abhisek

2017

Ravula, S. R., Narasimman, S. C., Wang, L., & Ukil, A. (2017). Experimental Validation of Leak and Water-ingression Detection in Low-Pressure Gas Pipeline Using Pressure and Flow Measurements. IEEE Sensors Journal, in press.

https://hdl.handle.net/10356/85400

https://doi.org/10.1109/JSEN.2017.2745577

Experimental Validation of Leak and Water-ingression Detection in Low-Pressure Gas Pipeline Using Pressure and Flow Measurements

Sugunakar Reddy Ravula, Srivathsan Chakaravarthi Narasimman, Libo Wang, Abhisek Ukil, *Senior Member, IEEE*

***Abstract*—In underground low-pressure gas distribution pipelines, ground water enters the pipeline through cracks. This is known as the water ingress problem, and it occurs predominantly in the monsoon season when the water table is high. This issue is currently detected based on complaints from the users. In order to arrive at an efficient and reliable processing technique, experimental results of pressure and flow on an existing low-pressure gas pipeline are reported in the present paper. Several experiments for leak location, severity of the leak, water ingression with various volumes of water followed by removal of water are conducted. Healthy network loading data collected over a 24 hr period is used to verify the robustness of the derived parameters for water ingression detection. The present technique can detect leaks easily with a leak valve opening of 30^o. Robust detection of water ingression with more than 10% of pipe volume is possible.**

***Index Terms*—Gas pipeline, Condition monitoring, Pressure, Flow, Water ingress, Parameter**

I. Introduction

PIPELINES are the safest and most efficient mode of transportation for fluids over long distances. Gas pipelines are generally operated at three pressure ranges, high, medium and low. Leaks are one of the biggest problems with pipelines and they can occur due to a variety of reasons such as loose pipe joints, corrosion, third party interference or natural disasters. There are many leak detection techniques currently in use, but the techniques that work for high-pressure pipelines do not hold true for low-pressure lines. The detection of leaks and other anomalies is particularly challenging at low-pressure range (2-50 kPa). This is the focus of this work to test the validity of the detection techniques.

Pipelines are operated at high pressure for long distance transmission, and at low pressure for distribution purposes. In most networks, the total length of low-pressure lines is typically higher. In Singapore, the length of low-pressure pipelines is roughly about 3000 km [1], organized in a meshed network form. For increasing the gas distribution resilience, it is vitally important to monitor this vast network in real-time using robust physical parameters.

Sugunakar Reddy Ravula, Srivathsan Chakaravarthi Narasimman and Libo Wang are with the Energy Research Institute(ERI@N), Nanyang Technological University, Singapore, (email:sugunakar,srivathsan.cn,LIBO@ntu.edu.sg).

Abhisek Ukil is with the School of Electrical and Electronics Engineering, Nanyang Technological University, Singapore, (email: aukil@ntu.edu.sg).

This work was supported by the energy innovation programme office (EIPO) through the national research foundation and Singapore energy market authority. Project LA/Contract No.: NRF2014EWT-EIRP003-002.

A. Literature review

Different approaches have been employed to solve the problem of leak in pipelines [2]–[4]. Campanella et.al. proposed using distributed fiber optics techniques for monitoring gas network [2]. Karkulali et.al. suggested using acoustic impact monitoring to detect leaks in low pressure pipelines [3]. Chraim et.al. used a wireless network comprising of 20 gas sensors over an area of 200 square meters for leak detection [4]. Monitoring the odorant concentration using gas sensors has also been tested in multiple cases [5], [6]. However, the parameters monitored in the aforementioned techniques are susceptible to change due to external factors, which could cause false alarms. Pressure and flow rate in the pipeline are a direct measure of the nature of flow in the pipeline. There have been other techniques employed to detect leaks in pipelines [7]–[11], however, those have not been applied for pressure range as low as 2 kPa. The low-pressure range is a significant challenge, where most of the transmission level detections methods are not directly applicable.

B. Water ingress problem

In Singapore, low-pressure pipelines are particularly susceptible to the water ingress problem. This occurs at places where the ground water table is high causing the water to enter the gas pipelines when a leak occurs. This does not occur at high or medium pressure level, since the water outside the pipe is at a lower pressure than the gas inside the pipeline, which keeps the water away when a leak occurs. According to SP groups report, more than 25 cases of water ingress occur in a year [1].

A water ingress detection and localization technique using DTS (distributed temperature sensing) to monitor the temperature profile of a pipe has been proposed [12], but the temperature profile could vary due to many reasons apart from water ingress. Since this detection technique employs temperature, it can be used only for metal pipes. A detection technique, which uses pressure and flow measurements, overcomes all the aforementioned problems and can be used to detect both leaks and water ingress. The experimental validation of this technique is presented in this paper.

The remainder of the paper has been organized as follows. Section II outlines the testbed setup on which the detection techniques were tested. Section III describes the simulation method and its results. Section IV describes the test procedures

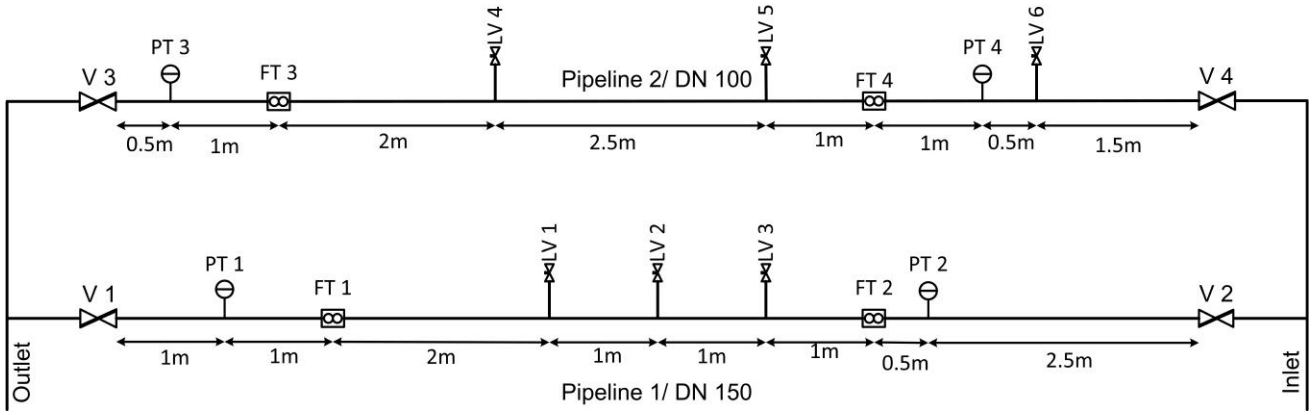

Fig. 1: Schematic of the experimental testbed

in detail. Section V presents the experimental results in details. Analysis of the results is discussed in section VI, followed by conclusion in section VII.

II. Experimental testbed setup

The experimental test bed is at SP Group's test site in Singapore, which can distribute town gas to household consumers. There is a 4-inch low-pressure regulator at the test bed, which tries to make the network pressure constant. The load is being shared by another regulator outside the testbed to ensure continuity in the gas supply to the consumers.

The test bed shown in Fig. 1 comprises of two ductile iron pipes, DN 150 and DN 100 with a length of 10m, which are connected in parallel. The gate valves (V1-V4) are connected at the outlet and inlet sides of both the pipelines to configure the network for parallel and isolated operation. Three ball valves, 2.54 cm in diameter are provided on each pipeline to simulate the leak scenario and for water ingression.

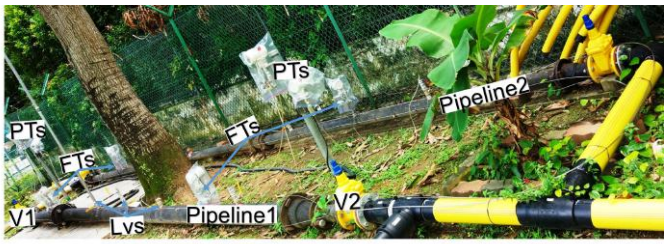

Fig. 2: Experimental testbed at Singapore

Intrinsically safe pressure transducers (PT1-PT4) and flow transducers (FT1-FT4) are installed near the ends of the pipelines. ABB pressure meter 266GSH is used for pressure measurement and the ABB differential pressure transducer 266DSH with an averaging type pitot tube (APT) is used for flow measurements [13], [14].

The averaging type Pitot tube with probe diameter 18.7mm (FT1&2) and 25mm (FT3 &4) was used, which has an overall accuracy of 1.5%. The FT1 & FT2 are rated at 3600 m3/h and FT3 & FT4 are rated 500 m3/h. The output update time is 25ms with damping adjusted to 1s.

A 4-20mA current signal generated by these meters is measured and recorded continuously with the ABB data logger RVG 200 [15]. A photograph of the experimental testbed with all measuring instruments is shown in Fig. 2.

TABLE I: Boundary conditions and fluid properties

Parameters	Value
Pressure at Regulator	2 kPa
Velocity at outlet	1.572 ms^{-1}
Pressure at leak outlet	0 kPa
Fluid density	0.69 kg m^{-3}
Fluid viscosity	2×10^{-5} Pa.s

III. Simulation studies

The computational fluid dynamic (CFD) simulation studies are performed in COMSOL Multiphysics using the CFD module. The simulations are performed in 2-D, by choosing k-ϵ turbulence model. The geometry is based on the dimensions of the actual testbed (Fig. 1). The pressure regulator is about 20 meters away from the inlet of the testbed. Testbed geometry with the mesh structure is shown in Fig. 3.

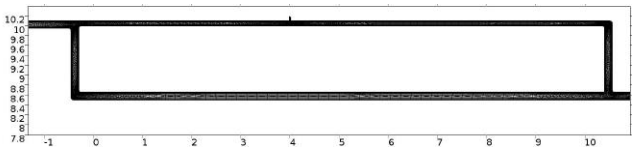

Fig. 3: Computation geometry with mesh structure

The pressure and velocity boundary conditions are calculated from the pressure and flow data of the network. Simulation parameters such as fluid properties and boundary conditions are show in Table I.

The average cross sectional pressure at locations close to the pressure transducers (PT1-PT4) are P1, P2, P3 and P4. The ratio of integral velocity to the diameter are calculated at locations close to the flow transducers (FT1-FT4) are V1, V2, V3 and V4.

The simulation results observed with a leak at Lv1 are shown in Table II. A pressure drop of 0.17kPa from about 2 kPa to 1.83 kPa is observed at all pressure locations when the leak valve is opened. This drop might be because of the regulator, which is 20m away from the inlet of testbed. The velocity at inlet of pipeline1 (V2), inlet and outlet (V3, V4) of

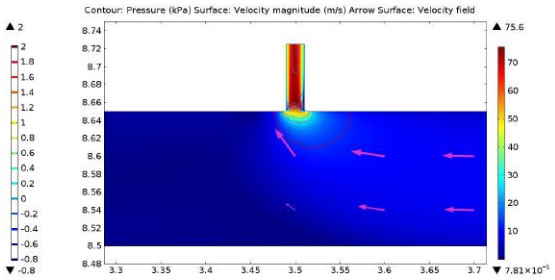

(a) Lv1

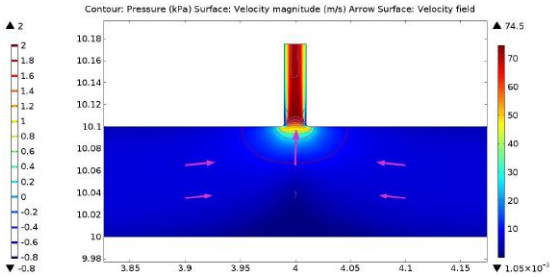

(b) Lv4

Fig. 4: Pressure and velocity at leak valves Lv1 and Lv4

the pipeline2 are higher when there is a leak compared with no leak case. This excess velocity is due to the gas escaping from the leak valve. However, the increase in velocity in the pipeline 2 is minimal compare to pipeline 1. The velocity at the outlet (V1) dropped because of the leak. There is no significant difference in pressure drop observed when the leak is simulated at different locations (Lv2-Lv6), since they are located close to each other.

The pressure and velocity distribution when leaks are at Lv1 and Lv4 is shown in Fig. 4. The dominant direction of flow at Lv1 is from the inlet of pipeline1. For Lv4, which is in pipeline2, the flow is from both sides of the pipe. This is because the pipeline1 has a greater diameter compared to pipeline2. Hence, the gas flows from the pipeline1 outlet through the pipeline2 outlet to Lv4.

IV. Test procedure

Various experiments are conducted in a controlled manner to mimic the real scenario of leak and water ingression in the gas pipeline network connected to the live gas distribution network in Singapore.

A. Leak test procedure for location and different angles

Leak test is conducted at all the leak valves (Lv1-Lv6) of both the pipelines. Three types of leak tests are conducted on these leak valves.

1) By quickly opening and closing the valve within 2 seconds,
2) By quickly opening the valve and holding for 30 seconds, then quickly closing it ,
3) By gradually opening the valve for 15 seconds and holding for 30 seconds then closing it for 15 seconds.

The leak test at various angles is conducted by connecting another ball valve above the leak valve. The leak valve is adjusted for various angles using an angle measuring instrument. The second ball valve is used to open and close the valve quickly with a holding period of 30 seconds.

B. Water ingress and removal procedure

Water ingression test is conducted through the leak valves by connecting a water hose. The amount of water in the pipeline is tracked by the volumetric water meter, which is connected in between the water tap and the leak valve. The water ingression test is conducted at various steps from 10% to 90% (effective volume of the pipeline at equal level of the pipeline 1 of approximately 270 liters is considered as 100% volume) with a holding time of 180s for each step.

After the pipe is fully blocked, the water from the pipeline is removed using water pumps. The pressure and flow data are recorded during water ingression and removal, to capture the overall signature.

V. Results

A. Leak test (varying position of leak)

The leak tests are conducted on all the six valves, with both the pipelines charged such that the influence of each valve can be recorded at all the meters. An increased flow rate is recorded at the flow meter upstream of the leak valve and decreases at the flow meter downstream with respective to the leak valve. For the tests on the first three valves, the flow variation in the second pipeline is very small when compared to the first pipeline and for the rest of the valves, the change in flow is significant for the second pipeline. The change in flow is subdued in the first pipeline for the final three leak valves compared to the second pipeline, which however is not as subdued as is the case with the second pipeline for the first three leak valves. The leak valve six alone produces a drop in both the inlet and the outlet flow meters since they are both located downstream of the leak valve.

The effect of a leak valve in the first pipeline on the flow rate in the second pipeline is much weaker than the effect of a leak valve on the second pipeline on the flow rate of the first pipeline. This is due to the difference in diameters of the pipelines. The inlet and outlet flow rates in the pipelines increase when the leak test is done at the adjacent pipeline. This also indicates that irrespective of the pipeline, the flow meters on the adjacent pipeline behave akin to the flow meter upstream with respective to the leak valve under test.

The leak test also indicates a difference between the pipelines in the region from which gas flows to compensate when a leak valve is opened. In the first pipeline, the increase in the inlet flow rate is lot higher than the decrease in the outlet flow rate and vice versa for the second pipeline. The difference in the direction of gas flow when a leak occurs between Lv1 and Lv4 is delineated in Fig. 4. This indicates that when the leak valve is opened in the second pipeline, the gas rushes into the pipeline from the outlet side. In the first pipeline, the gas flowing in from the inlet side is more than the gas flowing in from the outlet side.

TABLE II: Simulation data during leak and no leak

Pressure/Velocity	P1 kPa	P2 kPa	P3 kPa	P4 kPa	V1 m/s	V2 m/s	V3 m/s	V4 m/s
Leak at Lv1	1.838	1.833	1.838	1.839	0.21	8.05	2.04	2.04
Without leak	1.995	1.996	1.995	1.996	1.12	1.12	0.68	0.68

From Fig. 5, it can be observed that there are only two peaks observed for each set of three tests, since the instantaneous leak test does not produce significant changes in either pressure or flow. The pressure profile did not vary significantly due to the position of the leak valve on which the test is performed. The signature tapers gradually on either side for the test in which the leak valve is opened and closed gradually, whereas a steep drop and rise corresponding to the instantaneous opening and closing of the leak valve is observed. Such a differentiation is not observed in the case of flow rate for the leak tests. Hence, the detection of leaks is easier with flow meters, since they produce a significantly different signature depending on its location. The pressure at the pressure transmitters (PT1,PT2)with a leak at Lv1 is 1.82 kPa and the pressure when there is no leak is 1.99 kPa. These values are similar to the simulated results shown in table II. The overall trend of velocity observed experimentally is also similar to the simulation results but there is a discrepancy in the exact values, this is due to the characteristics of the regulator operating in parallel to the test setup.

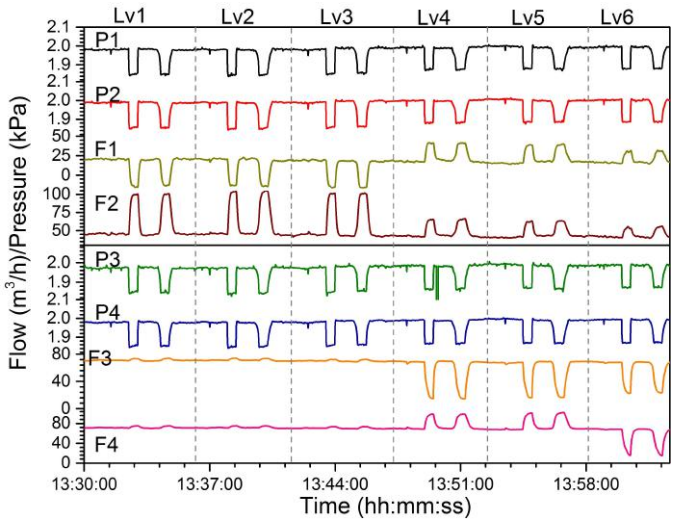

Fig. 5: Pressure and flow profiles during leak at various positions

B. Leak test (varying leak width)

The pressure signature shown in Fig. 6 is found to vary depending on the width of the leak that is simulated with the help of a leak (ball) valve opened to different angles. The drop in pressure increased as the angle of valve opening is increased. An increase in the inlet flow rate and a commensurate decrease in the outlet flow rate is observed when the leak valve is opened and the magnitude of change in flow rate is found to increase with the increase in angle of opening of the leak valve. The response in the pressure signals occurred as soon as the leak valve is opened, whereas in the case of the flow signals there is a delay before the effect of the leak valve opening is observed. The pressure at the inlet (Pressure 2) and the outlet (Pressure 1) are not equal as they should be, with the inlet pressure being a bit higher than the outlet pressure. This drop in pressure can be attributed to the friction in the pipeline.

The change in pressure and flow is not significant when the leak valve is positioned at 10^o , since the opening is very small due to the initial offset of the ball valve. Keeping in trend with the findings from the previous leak tests, this test is done on the first pipeline and the increase in the inlet flow rate is higher than the decrease in the outlet flow rate. The leaks start producing a clear identifiable pressure and flow signature from 30^o onwards. The detection of leaks gets easier as the width of the leak increases. The pressure is not indicative of the location of the leak, but the flow signature increases or decreases depending on the location of the leak with respect to the meter as in the previous case.

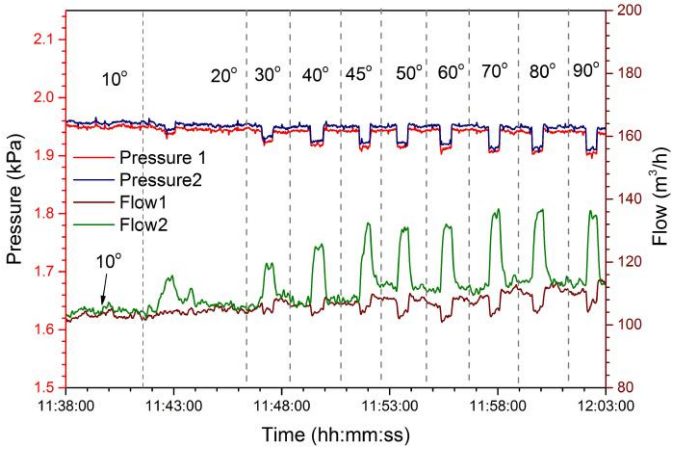

Fig. 6: Pressure and flow profiles by varying the width of leak

C. Water ingress different levels

The water ingress test described in the previous section is conducted on the leak valve Lv1 in the first pipeline. The pressure at the outlet and the amount of water in the first pipeline are plotted as a function of time in the Fig. 7. Initially there is no visible change in the pressure signal for the first 27 litres of water flowing into the pipeline. Pressure oscillations are visible when the water level in the pipe approaches 20% of its maximum capacity. The magnitude of oscillations increase with the water level inside the pipe. The magnitude of oscillation increases suddenly at water level approximately 50%. This pattern is similar for all the pressure meter readings. There is a pronounced correlation between the amount of water in the pipeline and the magnitude of oscillation in the

pressure signal during water ingress. The pressure signature during water ingress is vastly different from the signature during a leak, and therefore both can be differentiated and identified. Thus, the pressure transmitters can be used to detect the onset of water ingress in a pipeline, but they show no marked variation with the location of the water ingress in the pipeline.

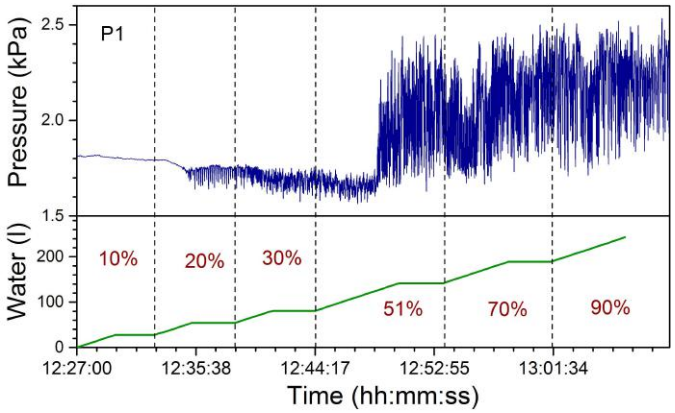

Fig. 7: Pressure profile for various levels of water ingression

D. Water ingress and removal

The water ingress test is conducted on the Lv5 in the second pipeline. Here, only the second pipeline is charged with the gas and the first pipeline is isolated. The isolation of the first pipeline is done using the gate valves V1 and V2. The pressure and flow profiles during the water ingression and the removal of water are shown in Fig. 8. Before the beginning of the water ingress, the inlet and outlet flow rates are almost equal while there is a small drop in pressure due to friction as mentioned earlier. The inlet and outlet pressures start increasing almost immediately, with the onset of water ingress. There is a sharp decrease in the inlet and outlet flow rates as soon as water ingress begins.

Oscillations are also observed, similar to the previous water ingress test. These oscillations are also visible in the flow readings. The pressure rises quickly and the oscillations stop, after the pipe is blocked, which can be identified from flow meter reading. The pressure stops increasing once the water ingression is stopped. There were two iterations of the water ingress test conducted leaving a three minute waiting period between them. The pressure and flow signature recorded during water ingress are vastly different from the leak test signals. Hence, differentiating leaks from water ingress is possible with the help of either pressure or flow readings. They also produce a unique and repeatable signature hence making the detection of the onset of water ingress possible. However, the point of entry of water can not be detected from these signals. Once the water ingress test is completed, a pump is connected to the lowest point in the pipeline system and started.

When water removal starts, the pressure drops immediately and again starts oscillating and eventually reaches values observed before the start of water ingress. Both the flow rates

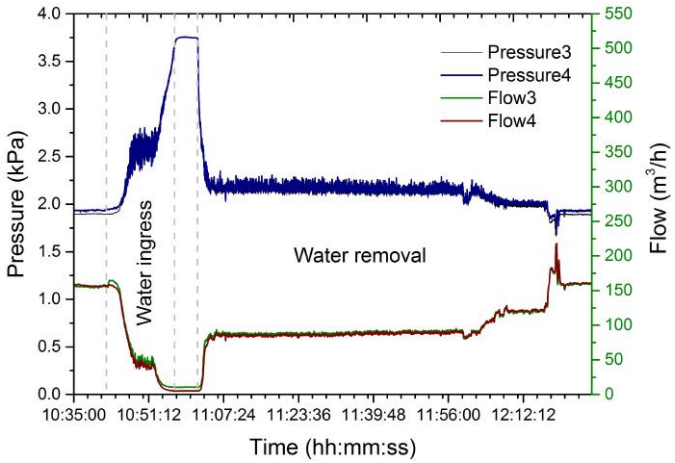

Fig. 8: Pressure and flow profiles during water ingression and water removal

from the pipeline start increasing and eventually reach the values observed before the start of water ingress. There is no marked difference between the inlet and outlet flow rates. The flow rates increase sharply almost immediately after the start of water removal. The oscillations in the pressure and flow are quite different from each other with the oscillations in pressure being far more pronounced than the oscillations in the flow rate. There is also an observable difference in the oscillations in pressure during water ingress and the oscillations during water removal. This will be helpful to identify the pipe sections affected when water is being removed from the syphon, which is where the water entering a section of the network is connected. The siphons are usually installed at the lowest points of a distribution network. The random spikes in the pressure and flow during water removal are also found to correspond to each other, hence indicating that the water thrashing inside the pipeline could cause these spikes. The pressure and flow values were found to revert back to their initial values observed before the start of the water ingress once the water in the pipeline was completely removed.

E. Water ingress network test

The water ingress test was conducted on Lv1 in the first pipeline and both the pipelines were charged. The pressure and flow signatures recorded from all the four meters are delineated in the Fig. 9. The oscillations in the pressure do not set in until much later in the water ingress test. The flow rate shows a different trend when compared to the previous results. In the first pipeline the inlet flow rate increases by a small margin initially and there is a proportional drop in the outlet flow rate. However, this is not as sharp as the signal change observed in the case of leaks. The rate of increase of the leak increases much greater than the rate of decrease in the outlet after some while. The inlet flow rate increases from about 100 m^3/hour to nearly 800 m^3/hour, which then decreases and increases only to decrease again all in the span of a few minutes. The outlet flow rate remains almost stable during this and the inlet stabilises once the pipeline is blocked.

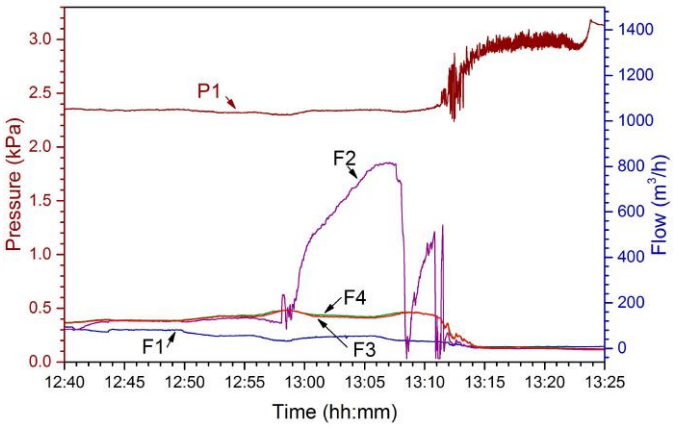

Fig. 9: Pressure and flow profiles for two pipelines during water ingression

When the water enters the second pipeline, the inlet and outlet flow rates at the second pipeline start decreasing and they decrease to zero quickly. The oscillations in pressure are observed when the first pipeline is blocked, after which there is a gradual increase in the pressure. There is no oscillation observed in the flow rate, and each of the individual flow rates seem to produce a different trend. This can be attributed to the fact that the flow meter used behaves differently based on the amount of water and whether water enters the high pressure tapping of the pitot tube. There is reducer in the first pipeline near the inlet flow meter, which accumulates water at the flow meter, causing the large variation in the inlet flow meter, while other meters remain fairly constant.

The oscillations in flow are observed for the previous experimental results however, they are not reproduced here. There are some recent promising flow meters, which can be used to accurately monitor the second phase medium. A new optical-based device for online black powder detection is proposed by Esra et al. [16] which functions using infrared(IR) light and determines the amount of different phases using chemo metric algorithms. Imran et al. [17] proposed a system which uses terahertz spectroscopy to analyse the electromagnetic properties of the contents of the pipeline such as absorbance and transmittance. Mahmoud et al. [18] proposed a system which analyses the acoustic and the impedance measurements of the medium to detect the presence and also quantify the two phase contents of a pipeline. However, since these solutions are not intrinsically safe and cannot be installed on the pipeline without disassembling the same, they cannot be applied to this problem currently.

However, the pressure oscillation has been observed in all experimental results and can be chosen as a stable feature to detect water ingress. The ratio of volume of water in the pipeline to the capacity of the pipeline has an influence on when the pressure signal starts oscillating after the onset of water ingress.

VI. Analysis of Results

The pressure and flow signatures are quite clear and indicative during leak. The water ingression creates oscillations both in pressure and flow. However, the pressure signal is found to be more reliable than the flow. It is important to identify a process parameter which is also indicative of the level of water ingression. Hence, various parameters derived from pressure data will be discussed for water ingression detection.

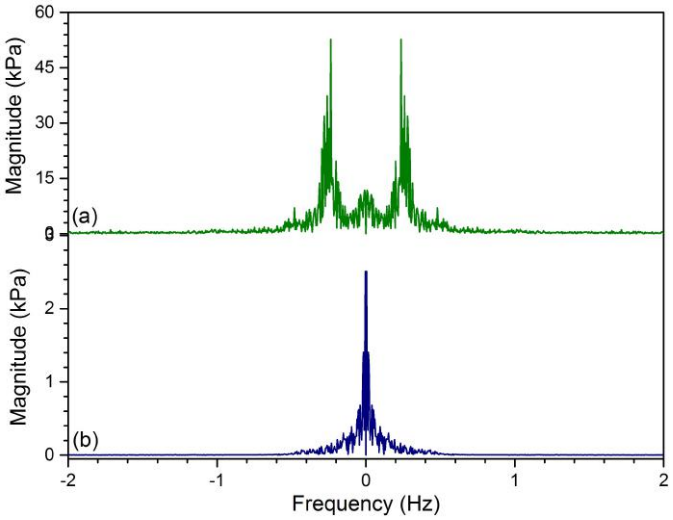

Fig. 10: Typical frequency domain plot (a) during water ingression and (b) without water ingression

The oscillations are found in the pressure signals during all of the water ingression experiments. Hence, frequency domain analysis is performed on the pressure signals using the Fast Fourier Transform (FFT), after subtracting the dominant dc component from the signal. Typical frequency domain plots of the pressure signals during and before the water ingress test are shown in Fig. 10. The pressure signal is quite steady before water ingression and hence, the dominant frequencies are near 0 Hz. In the case of water ingression, the dominant frequencies are slightly shifted from zero to the range of 0.2 to 0.5 Hz. However, this frequency band is not fixed and varies with the frequency of water oscillations due to the gas flow.

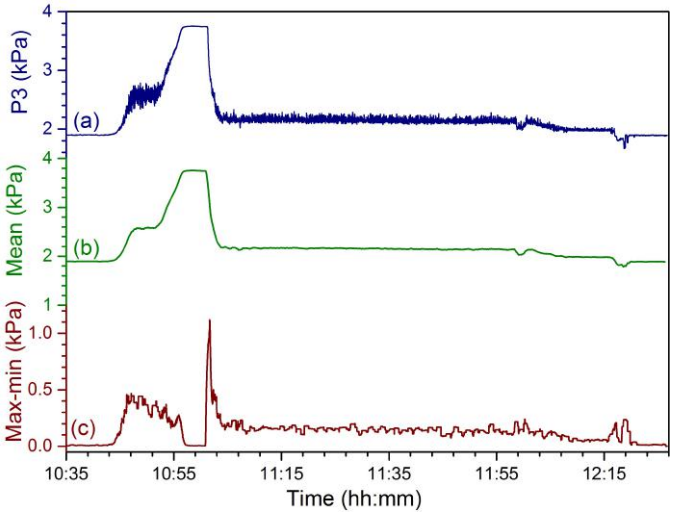

Fig. 11: (a) Pressure (b) Mean and (c) difference between maximum and minimum during water ingression and removal

Furthermore, the pressure signals are analysed in time domain with a fixed window size of 50 seconds, which is identified as the length of the characteristic signal based on observation. Mean and the difference between maximum and minimum of the pressure signal (P3) during water ingression and removal are shown in Fig. 11.

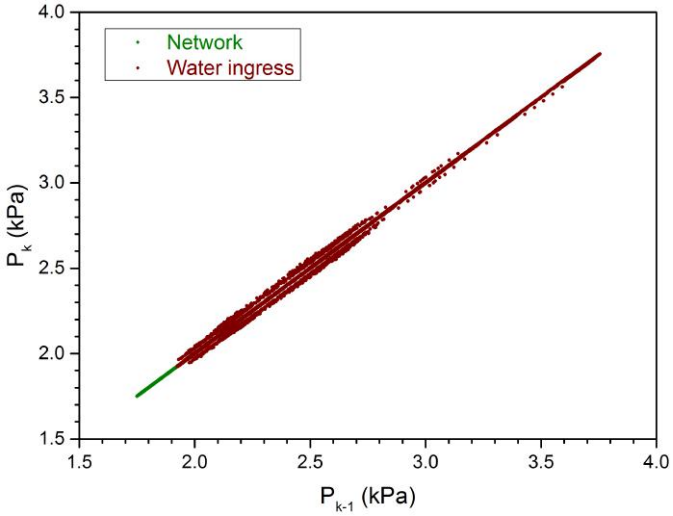

Fig. 12: Pressure variation plot during water ingression and during normal gas network loading

The mean pressure is around 1.9 kPa before water ingression and grows to about 2.5 kPa during water ingression. This is due to the reduction of effective cross section of the pipeline due to the seepage of water in the pipeline. After the pipe is blocked, the mean pressure steeply rises until the water ingression is stopped. The mean pressure steeply drops due to the water removal and returns to its normal mean of 1.9 kPa after the complete removal of water. This mean pressure can be used to detect water blockage in the pipe, during which pressure oscillations are not found. The difference between maximum and minimum values of pressure within 50 seconds window is indicative of oscillation magnitude, which is indicative of water ingression. However, this parameter is susceptible to outliers and random noise.

The plot between instantaneous pressure signal (P_k) and the one sample delayed pressure signal (P_{k-1}) is shown in Fig. 12. Under normal network loading condition, the plot is a straight line with a unity slope. This indicates that the pressure transition in normal condition is smooth, whereas in the case of water ingression, the points in the plot are scattered slightly away from unity slope. This is due to quick pressure transition during water ingression.

The root mean square error ($RMSE$) within the window ($N+1$ samples) between P_k and P_{k-1} is defined in eq. (1).

$$RMSE = \sqrt{\sum_{k=-N/2}^{N/2} \frac{(P_k - P_{k-1})^2}{N+1}}. \quad (1)$$

Another statistical parameter standard deviation (S_N) is calculated as

$$S_N = \sqrt{\frac{1}{N} \sum_{i=-N/2}^{N/2} \left(P_i - \overline{P}\right)^2}, \quad (2)$$

where, P_i is the instantaneous pressure and $\overline{P}$ is the mean pressure in the window.

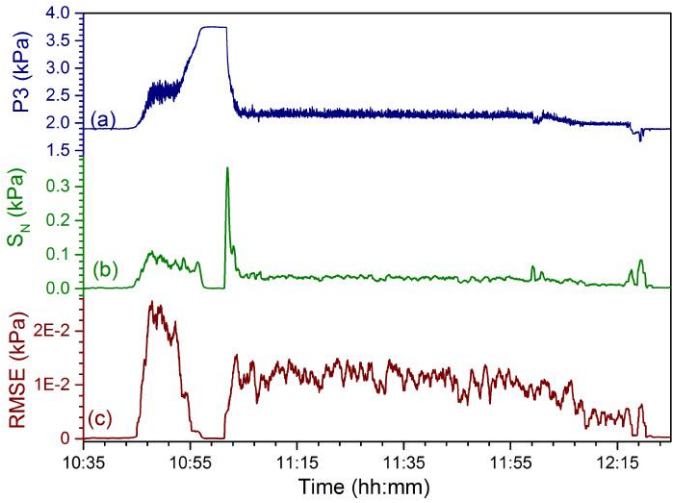

Fig. 13: Standard deviation and root mean square error during water ingression

These two parameters (S_N and $RMSE$) represent the variability in the signal. The standard deviation and the root mean square error calculated using moving window during water ingression and removal are shown in Fig. 13. The standard deviation and root mean squares errors are close to zero. Both of these quantities are quite indicative of steady oscillations in the pressure. During the start of water removal around 11:00, the pressure drops quickly from 3.8 kPa to 3 kPa within 50 seconds causing a spike in standard deviation although it's not an indicative of oscillation. The root mean square error does not show a higher value during this transition. This is due to a higher variation from the mean pressure but a smaller variation from the pressure at the previous instant.

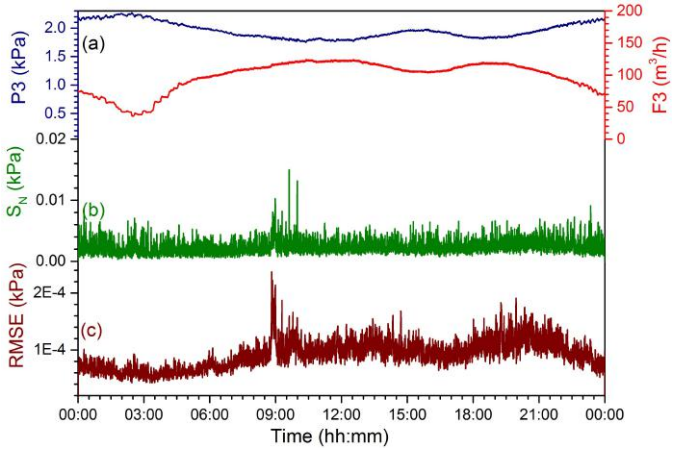

Fig. 14: Standard deviation and root mean square error during normal network operation

In order to identify the robustness of these parameters to avoid false positive detection, the S_N and $RMSE$ are calculated during normal operation of the network for a period of 24 hours. The standard deviation and $RMSE$ along with pressure and flow signals during normal network loading are shown in Fig. 14. It is observed that peak demands are around 13:00 and 19:00, with least demand being around 03:00. The pressure drops during high demand and rises during low demand. The variation in pressure and flow during normal network operation are smoother. The S_N and $RMSE$ are substantially lower than water ingression condition. Particularly, the $RMSE$ is 100 times lower than in case of water ingression.

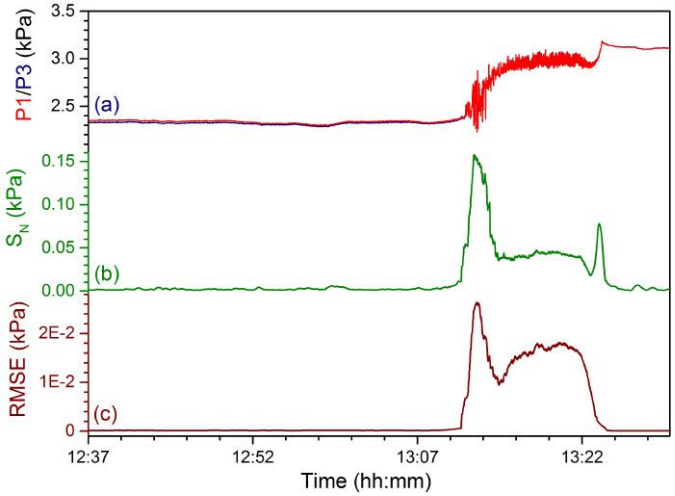

Fig. 15: Standard deviation and root mean square with the second pipeline

The parameters S_N and $RMSE$ are calculated for the pressure of the second pipeline (P3), when the water ingress is through Lv1 which is in pipeline 1. The pressures P1 and P3 shown in Fig. 15 are quite similar. The standard deviation and RMSE of the pressure from second pipeline are indicative of water ingression. There is a peak in the standard deviation at around 13:24 due to the pressure transition caused by the water blockage in the gas pipeline, which is not indicative of pressure oscillation.

In summary, overall water ingression detection system requires identification of water blockage using higher mean pressure or zero flow condition. The water ingression during unblocked flow situation creates a pressure oscillation which can be detected robustly using the derived variables, e.g. RMSE and standard deviation of the gas pressure. Moreover, the pressure signature is not intermittent, i.e., this can sustain as long as the leak and water ingression in the pipeline are not cleared.

VII. Conclusion

An experimental study is carried out for leak and water ingression detection in existing low pressure gas pipeline network. A Significant pressure drop has been identified during leak with an opening angle of 30^o. The flow at the inlet side increases during leak and decreases at outlet side due to the pressure drop. The reaction between water and gas creates oscillations in the pressure, which is a robust signature for water ingression. The pressure rises drastically when the pipe gets fully blocked with water. Both the leak and water ingression signatures are persistent till the problem gets cleared. Mean pressure and flow are the key indicators of the water blockage in the pipeline. The standard deviation and root mean square errors of pressure are key parameters for water ingression. Both the parameters are tested with network loading data of 24 hours. The root mean square error is the robust parameter for water ingression, which is 100 times larger than normal operating condition.

Acknowledgment

The authors thankfully acknowledge the technical support by the engineers of SP Group, Singapore.

References

[1] "Singapore power," http://www.singaporepower.com.sg, [Online; accessed 18-September-2016].

[2] C. E. Campanella, G. Ai, and A. Ukil, "Distributed fiber optics techniques for gas network monitoring," in *IEEE International Conference on Industrial Technology (ICIT)*, Taipei, Taiwan, Mar. 2016, pp. 646–651.

[3] P. Karkulali, H. Mishra, A. Ukil, and J. Dauwels, "Leak detection in gas distribution pipelines using acoustic impact monitoring," in *IEEE International Conference IECON 2016*. Institute of Electrical and Electronics Engineers (IEEE), Oct. 2016.

[4] F. Chraim, Y. Bugra Erol, and K. Pister, "Wireless gas leak detection and localization," *IEEE Transactions on Industrial Informatics*, vol. 12, no. 2, pp. 768–779, Apr. 2016.

[5] P. P. Neumann, D. Lazik, and M. Bartholmai, "Tomographic reconstruction of soil gas distribution from multiple gas sources based on sparse sampling," *IEEE Sensors Journal*, vol. 16, no. 11, pp. 4501–4508, Jun. 2016.

[6] C. Zanchettin, L. Maciel Almeida, and F. D. de Menezes, "An intelligent monitoring system for natural gas odorization," *IEEE Sensors Journal*, vol. 15, no. 1, pp. 425–433, Jan. 2015.

[7] A. Lay-Ekuakille and P. Vergallo, "Decimated signal diagonalization method for improved spectral leak detection in pipelines," *IEEE Sensors Journal*, vol. 14, no. 6, pp. 1741–1748, Jun. 2014.

[8] M. T. Humayun, R. Divan, L. Stan, D. Rosenmann, D. Gosztola, L. Gundel, P. A. Solomon, and I. Paprotny, "Ubiquitous low-cost functionalized multi-walled carbon nanotube sensors for distributed methane leak detection," *IEEE Sensors Journal*, vol. 16, no. 24, pp. 8692–8699, Dec. 2016.

[9] A. Lay-Ekuakille, G. Vendramin, and A. Trotta, "Robust spectral leak detection of complex pipelines using filter diagonalization method," *IEEE Sensors Journal*, vol. 9, no. 11, pp. 1605–1614, Nov. 2009.

[10] A. Cataldo, G. Cannazza, E. De Benedetto, and N. Giaquinto, "A new method for detecting leaks in underground water pipelines," *IEEE Sensors Journal*, vol. 12, no. 6, pp. 1660–1667, Jun. 2012.

[11] M. Meribout, "A wireless sensor network-based infrastructure for real-time and online pipeline inspection," *IEEE Sensors Journal*, vol. 11, no. 11, pp. 2966–2972, Nov. 2011.

[12] L. Wang, S. C. Narasimman, S. R. Ravula, and A. Ukil, "Water ingress detection in low-pressure gas pipelines using distributed temperature sensing system," *IEEE Sensors Journal*, vol. 17, no. 10, pp. 3165–3173, May 2017.

[13] *2600T series guage pressure transmitters 266GSH*, ABB, data sheet DS/266GSH/ASH-EN Rev. I.

[14] *2600T series differential pressure transmitters 266DSH*, ABB, data sheet DS/266DSH-EN Rev. H.

[15] *ScreenMaster RVG200 paperless recorder*, ABB, data sheet DS/RVG200-EN Rev. C.

[16] E. A. Hosani, M. Meribout, A. Al-Durra, K. Al-Wahedi, and S. Teniou, "A new optical-based device for online black powder detection in gas pipelines," *IEEE Transactions on Instrumentation and Measurement*, vol. 63, no. 9, pp. 2238–2252, Sep. 2014.

[17] I. M. Saied, M. Meribout, E. Kato, and X. H. Zhao, "Terahertz spectroscopy for measuring multiphase fractions," *IEEE Transactions on Terahertz Science and Technology*, vol. 7, no. 3, pp. 250–259, May 2017.

[18] M. Meribout, N. Al-Rawahi, A. Al-Naamany, A. Al-Bimani, K. Al-Busaidi, and A. Meribout, "Integration of impedance measurements with acoustic measurements for accurate two phase flow metering in case of high water-cut," *Flow Measurement and Instrumentation*, vol. 21, no. 1, pp. 8–19, 2010.

Sugunakar Reddy Ravula received the B.Tech degree in electrical and electronics engineering in 2007 and M.Tech degree in nanotechnolgy in 2009 from Jawaharlal Technological University, Hyderabad, India. He received Ph.D. degree from electrical engineering department, Indian Institute of Technology Madras, Chennai, India in 2015.He is currently working as Research Fellow at Nanyang Technological University, Singapore in advanced multi-sensor anomaly monitoring and analytics for gas pipeline. His research interests include nanomaterials, gas sensors, finite element analysis, condition monitoring, signal processing and data analytics.

Srivathsan Chakaravarthi Narasimman received the B.E. degree in electronics and instrumentation engineering from Anna University, Chennai, India, in 2015 and the M.Sc. degree in computer control and automation from the Nanyang Technological University, Singapore in 2016. Since 2016, he is a Research Associate in the Energy Research Institute at Nanyang Technological University, Singapore. His research interests include process instrumentation, data driven modelling and control theory.

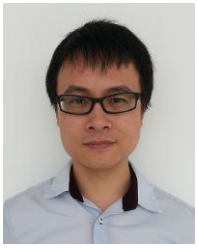

Libo Wang received the B.Eng degree in optical engineering from Zhejiang University, China, in 2007. He also received the Ph.D degree in Materials Science and Engineering from Nanyang Technological University, Singapore, in 2014. From 2008-2013, he was working as a project officer in school of Electrical and Electronic Engineering, NTU. After that, he joined Temasek Laboratories @NTU as a research scientist. Since 2016, he is a research fellow with Energy Research Institute @NTU, working on fiber-optics distributed temperature sensor for gas leak detection. His research interests include optical materials, high power laser system, smart sensors, condition monitoring, data processing and analysis.

Abhisek Ukil (S'05-M'06-SM'10) received the B.E. degree in electrical engineering from the Jadavpur Univ., Kolkata, India, in 2000 and the M.Sc. degree in electronic systems and engineering management from the Univ. of Bolton, Bolton, UK in 2004. He received the Ph.D. degree from the Pretoria (Tshwane) University of Technology, Pretoria, South Africa in 2006, working on automated disturbance analysis in power systems.

From 2006-2013, he was Principal Scientist at the ABB Corporate Research Center, Baden-Daettwil, Switzerland. Since 2013, he is Assistant Professor in the School of EEE, Nanyang Technological University, Singapore. He is inventor of 10 patents, and author of more than 100 refereed papers, a monograph, 2 chapters. His research interests include condition monitoring, smart grid, renewable energy, signal processing applications.